A Study on the Influence of Thermoplastic Extrusion Parameters and Annealing Post-Processing on the Technical Tensile Properties and Productivity of the Additive Manufacturing Process

Dragos Valentin Iacob
Department of Mechanical Engineering, Doctoral School, Petroleum-Gas University, Ploiesti, Romania
dragoshicb@gmail.com

Dragos Gabriel Zisopol
Mechanical Engineering Department, Petroleum-Gas University, Ploiesti, Romania
zisopold@upg-ploiesti.ro (corresponding author)

Mihail Minescu
Mechanical Engineering Department, Petroleum-Gas University, Ploiesti, Romania
mminescu@upg-ploiesti.ro

Received: 16 April 2026 | Revised: 31 May 2026 | Accepted: 8 June 2026

ABSTRACT

This study examines the influence of thermoplastic extrusion parameters and post-processing via annealing on the tensile mechanical properties and productivity of the additive manufacturing process. The 27 tensile test specimens were additively manufactured from recycled PETG filament (rPETG) on a QIDI Q1 Pro 3D printer using a layer height L_h of 0.10 to 0.20 mm and an infill density of I_d of 50 to 100%. The tensile specimens were heat-treated at a temperature of 75 °C for 180 min, with slow cooling. A total of 27 specimens were prepared using thermoplastic extrusion and heat-treatment, followed by testing on the Barrus White 20 kN machine to determine their tensile properties, including tensile strength, percentage elongation at break, and modulus of elasticity. The results indicate that pre-processing significantly influences the tensile properties of the specimens, with I_d having the dominant influence. The fundamental principle of value analysis was applied to study the cost-effectiveness and the impact of heat treatment on productivity. The findings suggest that annealing heat treatment negatively affects productivity.

Keywords-3D printing; thermoplastic extrusion; printing parameters; tensile; value analysis; annealing

I. INTRODUCTION

The evolution of additive manufacturing technologies, with rapid prototyping, has enabled the development of effective solutions for the manufacture of functional components in leading industrial fields such as aerospace, defense, machine building, medical, armament, and defense industries [1-5]. Additive manufacturing by thermoplastic extrusion outperforms other methods due to its accessibility, diversified range of materials, and ease of use [6-8]. However, the specific technology has several disadvantages, including the anisotropic nature of the mechanical properties and the long execution time of the parts.

Productivity is a crucial performance indicator of all manufacturing processes. In thermoplastic extrusion additive manufacturing, common strategies for enhancing productivity aim at increasing the layer height deposited per pass (L_h), the printing speed (V_p), and decreasing infill density (I_d) or optimizing the internal structure [9-13]. Systematic optimization of process parameters, such as layer height, fill density, print speed, fill pattern, or nozzle diameter, is effective in increasing the productivity of additive manufacturing by thermoplastic extrusion [14-17]. Optimizing additive manufacturing parameters reduces the defect rate in the production type and enhances the mechanical performance of the printed components by increasing the interlayer adhesion and thermal fusion between successively deposited layers [18-

20]. Another strategy for improving the mechanical and quality performance of parts made using additive technologies is to implement machine learning, which, in additive manufacturing, helps increase the sustainability and competitiveness of additive technologies [21-23]. Moreover, post-processing by annealing heat treatment increases the fusion between layers and improves mechanical performance, while the residual stresses accumulated during additive manufacturing are allowed to relax, and the fusion between layers is improved [24-26].

The application and influence of post-processing by thermal annealing on mechanical characteristics have been investigated. Authors in [24] analyzed the effects of printing parameters and modern post-processing methods (thermal treatment, ultrasound treatment) on structural defects. Their results indicated that the mechanical properties depend on the material deposition angle, layer thickness, and nozzle temperature. Post-processing by thermal treatment leads to a reduction of internal stresses and improves the crystallinity of the polymer. In [25], the influence of three key parameters (deposited layer height, infill density, and heat treatment duration) on mechanical characteristics was analyzed. It was demonstrated that the strength of the parts is significantly influenced by the deposited layer thickness and filling density, with heat treatment generating a minor improvement. Authors in [26] explored the influence of heat treatment on the tensile strength of PLA specimens. The tensile specimens were subjected to temperatures of 55, 65, 80, and 95 °C for 15 h, followed by slow cooling. It was shown that the pieces treated at 95 °C suffered significant deformation and could not be used for tensile strength determinations. For the temperature of 65 °C, the tensile strength increased by 29%, and at 80 °C, the tensile strength increased by 32%. The Shore D hardnesses were in the range of 80-83, indicating that the heat treatment does not influence surface hardness.

The present study examines the influence of additive manufacturing parameters due to thermoplastic extrusion with layer height deposited in one pass (L_h = 0.10 to 0.20 mm), filling density (I_d = 50 to 100%), and annealing heat treatment on the technical performance of specimens manufactured by thermoplastic extrusion of recycled PETG (rPETG) filament. The novelty of this study lies in the integration of recycled materials within additive manufacturing, the use of post-processing through heat treatment, and the integration of value analysis to optimize costs, performance, and resources.

II. INFLUENCE OF THERMOPLASTIC EXTRUSION

A. *Additive Manufacturing of Tensile Test Specimens*

In the first step, a 3D model of the part was modeled using Solidworks 2023 CAD software, and a tensile test specimen was manufactured in accordance with the ISO 527-1:2019 standard [27, 28]. The 3D model of the tensile specimen was converted to STL format and subsequently processed in the QIDI Slicer software. 9 G-Code files were generated for the manufacture of tensile specimens from Everfil brand rPETG. According to the manufacturer's specification sheet, the filaments have a diameter of 1.75 mm, a diameter tolerance of ±0.02 mm, a thermal conductivity of 0.2 W/m °C, a Vicat softening temperature (rate B/50) of 97 °C, a relative temperature index (electrical) of 130 °C, a glass transition temperature of 80 °C, and a density of 1.29 g/cm^3 [29]. Figure 1 illustrates the shape and dimensions of the tensile specimen, while Table I presents the manufacturing parameters. The thermoplastic extrusion parameters were selected based on the manufacturer's recommendations and the slicer profile.

Fig. 1. Tensile sample shape and dimensions in SolidWorks 2023.

TABLE I. TERMOPLASTIC EXTRUSION PARAMETERS

Variable printing parameters	Constant printing parameters
Layer height, L_h =0.10, 0.15, and 0.20 mm	Equipment: QIDI Q1 Pro
	Material: rPETG
	Printing speed: P_s = 120 mm/s
	Extrusion temperature: E_t =250 °C
Infill density percentage, I_d =50, 75, and 100 %	Platform temperature: P_t =70 °C
	Infill pattern: I_p = Grid
	Plate adhesion: P_a = brim
	Extrusion width: E_w = 0.42 mm

A Taguchi L9 design was used for the experimental design, which ensures statistical relevance. Three replicates were performed for each type of configuration. The 9 G-Code files, containing the work instructions for manufacturing tensile specimens from rPETG filament, were transferred to the QIDI Q1 Pro 3D printer, as shown in Figure 2. A total of 27 tensile specimens were manufactured. Figure 3 shows tensile specimens manufactured from rPETG filament by thermoplastic extrusion on the QIDI Q1 Pro 3D printer.

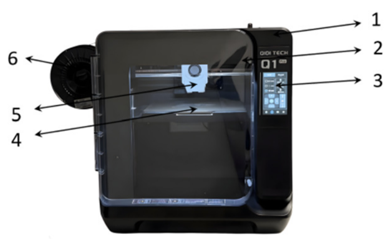

Fig. 2. QIDI Q1 Pro 3D printer: 1 – frame, 2 – access door, 3 – control display, 4 – platform, 5 – print head, 6 – filament spool.

B. *Post-Processing of Tensile Specimens*

Post-processing is an intermediate operation that takes place after the additive manufacturing is completed, and before the final use of the part. In this study, post-processing includes subjecting the tensile specimens to heat treatment for improvement. The heat treatment parameters were chosen considering the minimum deformation of the parts, based on [30]. The samples were subjected to heat treatment at 75 °C for 180 min [30].

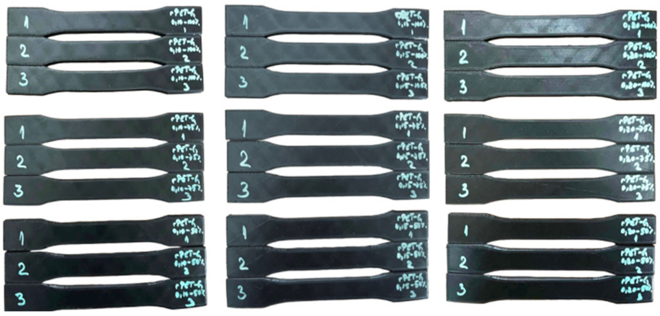

Fig. 3. Tensile specimens additively manufactured on the QIDI Q1 Pro 3D printer from rPETG filament.

(a)

(b)

Fig. 4. Equipment and parts used for heat treatment: (a) electric oven, (b) tensile specimens additively manufactured from rPETG.

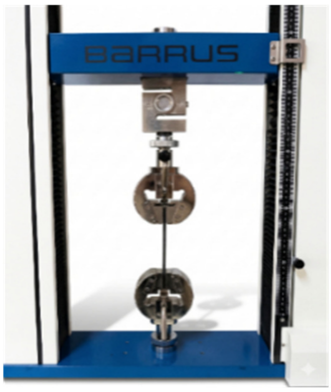

Fig. 5. Tensile testing of additively manufactured and heat-treated rPETG specimens.

C. Determination of Tensile Characteristics of Specimens

To determine the tensile characteristics of the 27 additively manufactured and heat-treated rPETG specimens, a Barrus White 20 kN machine was used. Tensile tests were performed according to the ISO 527:2019 standard, using a speed of 5 mm/min, as displayed in Figure 5. During the tests, the laboratory temperature and humidity were maintained at 22 °C and 52%, respectively. Figure 6 shows the 27 rPETG specimens after tensile testing on the Barrus White 20 kN machine.

Fig. 6. Tensile specimens additively manufactured from rPETG and heat-treated after tensile testing on the Barrus White 20 kN machine.

III. RESULTS

After the tensile tests, percentage elongation at break and modulus of elasticity were also determined. The test results are depicted in Figures 7-9.

(a)

(b)

(c)

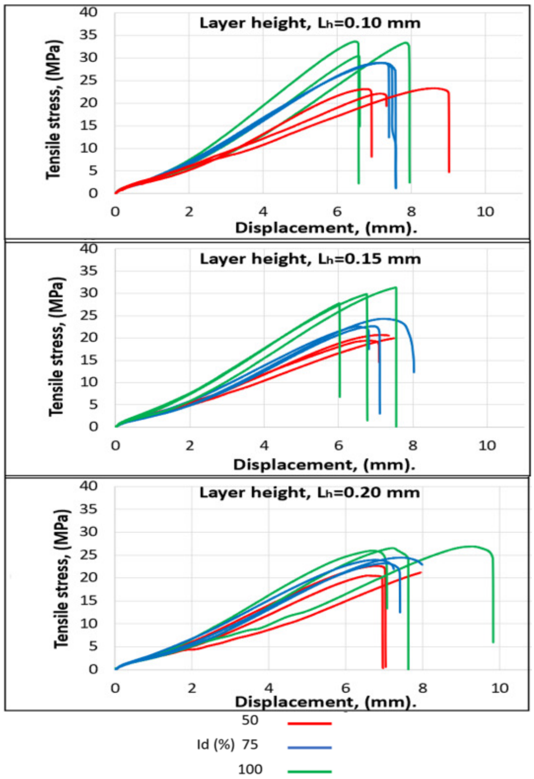

Fig. 7. Tensile stress-displacement graphs of heat-treated tensile specimens additively manufactured from rPETG, at : (a) L_h =0.10 mm, (b) L_h = 0.15 mm, and (c) L_h = 0.20 mm.

The maximum average breaking strength was obtained for the set of specimens manufactured with L_h = 0.10 mm and I_d = 100%, and the minimum average breaking strength was obtained for the set of specimens manufactured with L_h = 0.15 mm and I_d = 50%. As shown in Figure 7(a) increasing the filling density (I_d) from 50% to 75%, increased the breaking strength by 5.66-6.77 MPa, representing a percentage increase of 24.31% to 30.63%. Increasing I_d from 75% to 100% resulted in an increase in tensile strength by 1.52-4.59 MPa (5.27%-16.20%). Similarly, as presented in Figure 7(b), by increasing I_d from 50% to 75%, tensile strength increased by 3.20-3.64 MPa (16.46%-17.59%). While increasing I_d from 75% to 100% resulted in an increase in tensile strength by 5.20-7.04 MPa (23.01%-28.95%). Figure 7(c) indicates a similar pattern. An increase in filling density from 50% to 75%, increased the tensile strength by 1.81-2.66 MPa (8.01%-12.96%), while increasing the I_d value from 75% to 100% led to an increase in the tensile strength by 2.43-2.79 MPa (9.94%-12.02%).

(a)
(b)
(c)

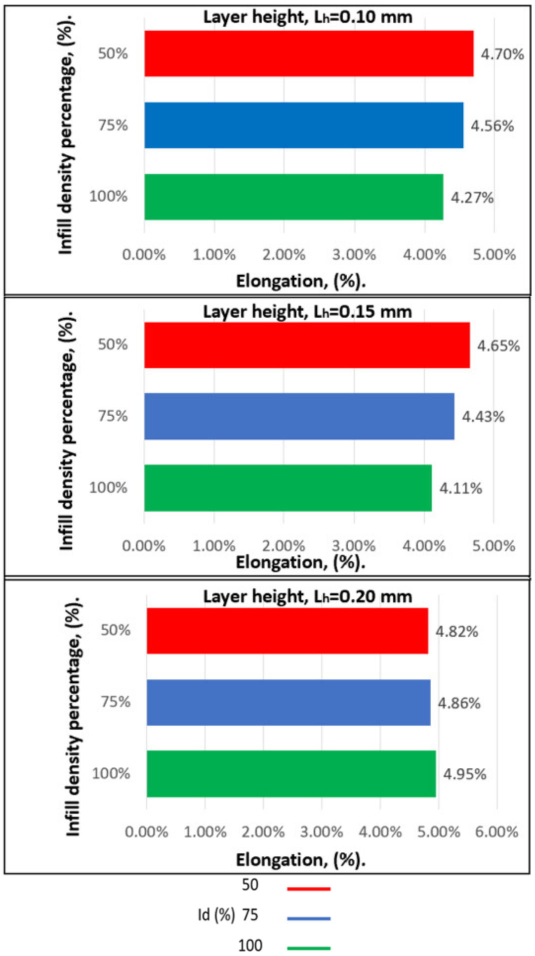

Fig. 8. Average percentage elongations at break of heat-treated tensile specimens additively manufactured from rPETG, at: (a) L_h = 0.10 mm, (b) L_h = 0.15 mm, (c) L_h = 0.20 mm.

Figure 8 illustrates the average values of the percentage elongations at break of heat-treated tensile specimens manufactured by additive thermoplastic extrusion of the rPETG filament. For L_h = 0.10 mm, an increase in I_d from 50% to 75% and from 75% to 100% led to a decrease in the average elongations at break of the tensile specimens by 3.07% and 6.31%, respectively, as shown in Figure 8(a). For L_h = 0.15 mm, a similar behavior was observed; that is, the increase in I_d from 50% to 75% and subsequently from 75% to 100% led to a decrease in the percentage elongations at break by 4.71% and 6.31%, respectively. However, for L_h = 0.20 mm, a different response was observed: increasing I_d to 75% led to a decrease in the average elongations at break by 0.83%, and increasing I_d from 75% to 100% led to an increase in the average elongations at break by 1.98%.

Figure 9 depicts the average values of the elastic modulus corresponding to the heat-treated tensile specimens additively manufactured by thermoplastic extrusion of rPETG. The highest values of the elastic modulus (0.49-0.77 GPa) were obtained for the additively manufactured rPETG specimens with L_h = 0.10 mm. For L_h = 0.10 mm, increasing the percentage filling density value from 50% to 75% and subsequently from 75% to 100% led to an increase in the elastic modulus by 17.40-47.50 % and 10.23-30.71%, respectively. For L_h = 0.15 mm, increasing I_d from 50% to 75% and subsequently from 75% to 100%, increased the elastic modulus by 19.13-21.18% and 37.10-38.98) %, respectively. Similarly, for L_h = 0.20 mm, the gradual increase of I_d from 50% to 75% and from 75% to 100% resulted in an increase of the elastic modulus by 2.82-20.86 % and 11.10 %, respectively. The low values of the modulus of elasticity are the result of micro-gaps between the layers that reduce the actual cross-sectional area.

(a)
(b)
(c)

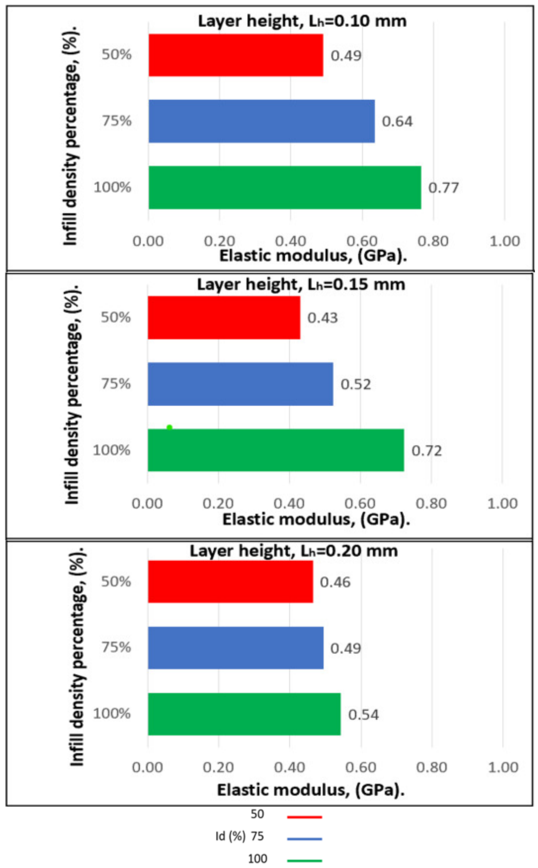

Fig. 9. Average elasticity modulus corresponding to heat-treated tensile specimens additively manufactured from rPETG, at: (a) L_h = 0.10 mm, (b) L_h = 0.15 mm, and (c) L_h = 0.20 mm.

A. Evaluation and Optimization of Thermoplastic Extrusion Parameters for rPETG

Minitab software version 20.1 [31] was used to evaluate and optimize the variable parameters of thermoplastic extrusion at L_h = 0.10, 0.15, and 0.20 mm, and I_d = 50, 75, and 100% for the manufacture of rPETG tensile specimens. Table II summarizes the data obtained from the Analysis of Variance (ANOVA).

The ANOVA results indicate that I_d is the most significant parameter with a contribution of 69.40% (p-value = 0.012), while L_h does not significantly influence the tensile strength values of the specimens manufactured from PETG and rPETG, which have a contribution of 22.25%. For this reason, increasing L_h helps reduce the printing time and costs associated with electricity, without significantly affecting the mechanical characteristics.

TABLE II. RESULTS OF ANOVA ANALYSIS.

Source	DF	Contribution (%)	F-value	p-value
L_h (mm)	2	22.25%	5.33	0.074
I_d (%)	2	69.40%	16.63	0.012
Error	4	8.35%	-	-
Total	8	100%	-	-

Figure 10 portrays the Pareto chart, highlighting the influence of the thermoplastic extrusion parameters on the tensile strengths of rPETG tensile specimens. The statistical influence value of the parameter $B = I_d$ is 5.617 units, and that of the parameter $A = L_h$ is 2.839. This suggests that the parameter $B = I_d$ has a 97.85% greater influence than the parameter $A = L_h$. Figure 11 shows the optimization chart of the thermoplastic extrusion parameters for the manufacture of rPETG tensile specimens. The purpose of the optimization is to maximize tensile strength.

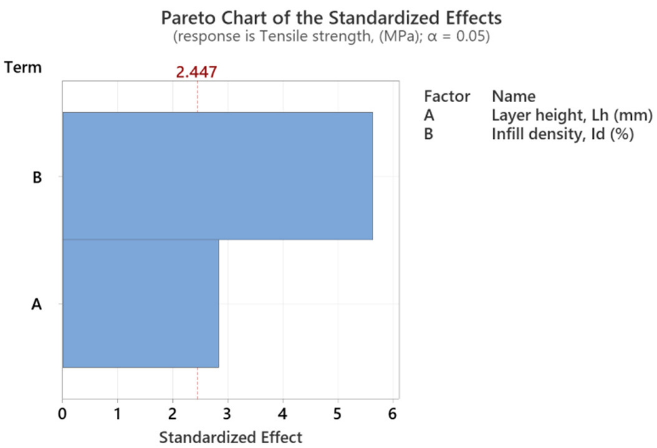

Fig. 10. Pareto chart of the influence of variable thermoplastic extrusion parameters ($A = Lh$ and $B = Id$) on the breaking strengths of tensile specimens manufactured from rPETG.

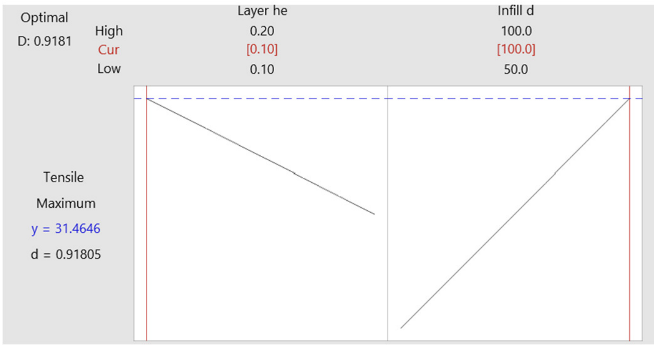

Fig. 11. Optimization graphs of variable thermoplastic extrusion parameters for maximizing the breaking strengths of additively manufactured rPETG specimens.

Considering the manufacturing parameters used in the current study, as shown in Table I, the optimization graphs in Figure 11 lead to the following optimal settings: L_h = 0.10 mm and I_d = 100%.

IV. INFLUENCE OF ANNEALING HEAT TREATMENT ON PRODUCTIVITY

To evaluate the cost-effectiveness of applying the annealing heat treatment on productivity, the fundamental principle of value analysis was used, which consists of maximizing the ratio between the utility value (V_i – tensile strength) and the production cost (C_p) [32].

$$\frac{V_i}{C_p} \rightarrow max. \quad (1)$$

The production cost (C_p) was determined as:

$$C_p = Q_{mat} \times P_{mat} + P_d \times E_c \times P_{en} + A_t \times E_c \times P_{en} \quad (2)$$

where C_p represents the production cost, Q_{mat} represents the material consumption, P_m is the material price (23.76 Euro/Kg), P_t is the printing time, E_c is the energy consumption (0.23 kWh), P_{en} is the electricity price (0.31 Euro/kWh), and A_t is the heat treatment time. The cost of energy is based on the standard commercial rates, while the price of the material is represented by the price actually paid by the authors.

Table III presents the $\frac{V_i}{C_p}$ ratio based on the tensile strength results for the 27 tensile test specimens made of rPETG and heat-treated (rPETG A), as well as the tensile strength results for the 27 tensile test specimens made of rPETG in [33].

TABLE III. DETERMINATION OF THE $\frac{V_i}{C_p}$ RATIO

rPETG			rPETG (A)		
V_i	C_p	$\frac{V_i}{C_p}$	V_i	C_p	$\frac{V_i}{C_p}$
MPa	Euro	MPa/Euro	MPa	Euro	MPa/Euro
28.03	9.82	2.85	25.49	10.41	2.42

The return on performance was calculated as:

$$R_p = \frac{\Delta\sigma}{\Delta C} \quad (3)$$

where R_p represents the return on performance, $\Delta\sigma$ is the difference between the average tensile strength of heat-treated specimens and the average tensile strength of untreated specimens, and ΔC is the difference between the production cost that includes heat treatment and the production cost without heat treatment. Using data from Table II and (3):

$$R_p = \frac{25.49-28.03}{10.41-9.82} = -4.305$$

The cost analysis showed that heat treatment does not add value, as the $\frac{V_i}{C_p}$ ratio is 0.43 (MPa/Euro) lower than that of the untreated tensile test specimens. The result of the cost-benefit analysis (-4.305) confirms that heat treatment reduces productivity and increases production cost without justifying the increase in mechanical performance.

V. CONCLUSION

This study examines the influence of thermoplastic extrusion parameters, including single-pass layer height (L_h = 0.10-0.20 mm) and fill density (I_d = 50–100%), on the tensile properties and the productivity of the additively manufactured specimen. The specimen was subjected to post-processing by annealing at 75 °C for a duration of 180 min. Twenty-seven tensile test specimens were additively manufactured on the QIDI Q1 Pro 3D printer by extruding rPETG filament. All 27 specimens were heat-treated and subsequently tested for tensile strength on the Barrus White universal testing machine, with a capacity of 20 kN. The highest average tensile strengths were recorded for specimens manufactured with an L_h of 0.10 mm and an I_d of 100%, while the lowest average tensile strength was recorded for specimens manufactured with an L_h of 0.15 mm and an I_d of 50%.

For L_h =0.10 mm, a sequential increase in I_d by 25%, starting from 50%, resulted in an increase in tensile strength of 26.67% and 12.29%, a decrease in percentage elongation at break by 3.07% and 6.31%, and an increase in elastic modulus by 29.21% and 20.58%. For L_h = 0.15 mm, the sequential increase in I_d by 25% starting from 50% resulted in an increase in tensile strength of 15.72% and 27.96%, a decrease in percentage elongation at break by 4.71% and 7.28%, and an increase in the elastic modulus by 21.50% and 38.19%. For L_h = 0.20 mm, the sequential increase of I_d by 25%, starting from 50%, resulted in an increase in tensile strength by 9.05% and 10.87%, an increase in percentage elongation at break by 0.83% and 1.98%, and an increase in the elastic modulus by 6.27% and 10.14%. The modulus of elasticity is influenced by the fill density and layer height: setting I_d =100% ensures a continuous cross-sectional area that efficiently transfers tensile stresses. The highest modulus of elasticity was achieved with L_h = 0.10 mm and I_d =100%. This performance can be attributed to the pressure exerted by the nozzle at the time of depositing the layers of material, which determines the molecular orientation. Reducing the L_h and I_d values produces a higher elongation at break since the thermoplastic yarns have the geometric freedom to deform.

The evaluation and optimization of thermoplastic extrusion parameters for the manufacture of rPETG tensile test specimens were performed in Minitab. The optimization analysis suggests that the percentage fill density (I_d) is the most significant parameter influencing the tensile strength of the test specimens. The highest tensile strength was obtained with an L_h of 0.10 mm and an I_d of 100%. Using the fundamental principle of value analysis (maximizing the ratio of utility value to production cost), the cost-effectiveness and the influence of heat treatment on productivity were determined. The strength-to-cost ratio (V_i/C_p) for the test specimens made of rPETG with heat-treated is 17.73% lower than that of the specimens made of rPETG. However, the rPETG samples were not heat-treated. Regarding mechanical performance and production time, an L_h of 0.20 and an I_d of 50% were found to be the optimal process parameters. However, from the strength-to-cost ratio point of view, an L_h of 0.10 and an I_d of 75% were the optimal process parameters.

Future research will focus on extending the study to other types of mechanical tests, as well as investigating the influence of heat treatment on dimensional accuracy, in addition to the influence of other parameters (printing speed and extrusion temperature). In future work, the authors aim to use these printing and heat treatment parameters for the manufacture of PETG and rPETG protections in the automotive industry.

DECLARATION OF COMPETING INTERESTS

The authors declare no competing interests.

ACKNOWLEDGMENT

The authors declare that no external funding was received for this work.

DATA AVAILABILITY

Not applicable to this work.

REFERENCES

[1] K. Chrz, J. Bruthans, and J. Ptáčník, "Clinical Application of FDM 3D Printing in Surgery and Traumatology: A Systematic Review," *Annals of Biomedical Engineering*, Feb. 2026, https://doi.org/10.1007/s10439-026-04021-z.

[2] R. H. Ibrahim and H. Salman, "Manufacturing of Polymer-Based Composite Material by FDM: Challenges and Opportunities for Functional Parts Design," *Next Materials*, vol. 10, Jan. 2026, Art. no. 101571, https://doi.org/10.1016/j.nxmate.2025.101571.

[3] R. C, R. Shanmugam, M. Ramoni, and G. BK, "A review on additive manufacturing for aerospace application," *Materials Research Express*, vol. 11, no. 2, Oct. 2024, Art. no. 022001, https://doi.org/10.1088/2053-1591/ad21ad.

[4] Y. Mohseni *et al.*, "Investigating Impacts of FDM Printing Parameters and Geometrical Features on Void Formation in 3D Printed Automotive Components," *Materials Today: Proceedings*, Jun. 2023, Art. no. S2214785323034508, https://doi.org/10.1016/j.matpr.2023.06.078.

[5] K. M. Hernandez, S. O'Brien, A. Bischoff, J. Parmigiani, and D. J. Roach, "Influence of 3D printing parameters on ULTEM 9085 mechanical properties using experimentation and machine learning," *npj Advanced Manufacturing*, vol. 2, no. 1, Sep. 2025, Art. no. 41, https://doi.org/10.1038/s44334-025-00049-6.

[6] C. R. Tripathy, R. K. Sharma, and V. K. Rattan, "An investigation on mechanical strength of fused filament fabricated and injection molded ASA parts," *Journal of Micromanufacturing*, vol. 8, no. 1, pp. 44–59, May 2025, https://doi.org/10.1177/25165984241306797.

[7] M. Lay, N. L. N. Thajudin, Z. A. A. Hamid, A. Rusli, M. K. Abdullah, and R. K. Shuib, "Comparison of Physical and Mechanical Properties of PLA, ABS and Nylon 6 Fabricated Using Fused Deposition Modeling

and Injection Molding," *Composites Part B: Engineering*, vol. 176, Nov. 2019, Art. no. 107341, https://doi.org/10.1016/j.compositesb.2019.107341.

[8] B. Podsiadły, A. Skalski, W. Rozpiórski, and M. Słoma, "Are We Able to Print Components as Strong as Injection Molded? —Comparing the Properties of 3D Printed and Injection Molded Components Made from ABS Thermoplastic," *Applied Sciences*, vol. 11, no. 15, Jul. 2021, Art. no. 6946, https://doi.org/10.3390/app11156946.

[9] C. Camposeco-Negrete, "Optimization of FDM Parameters for Improving Part Quality, Productivity and Sustainability of the Process Using Taguchi Methodology and Desirability Approach," *Progress in Additive Manufacturing*, vol. 5, no. 1, pp. 59–65, Mar. 2020, https://doi.org/10.1007/s40964-020-00115-9.

[10] G. Kónya, "Investigating the Impact of Productivity on Surface Roughness and Dimensional Accuracy in FDM 3D Printing," *Periodica Polytechnica Transportation Engineering*, vol. 52, no. 2, pp. 128–133, Feb. 2024, https://doi.org/10.3311/PPtr.22952.

[11] R. Kumaresan *et al.*, "Optimization of Inter-Layer Printing Parameters for Enhanced Mechanical Performance of PETG in Fused Deposition Modeling (FDM)," *Results in Engineering*, vol. 25, Mar. 2025, Art. no. 104564, https://doi.org/10.1016/j.rineng.2025.104564.

[12] D. D. Ardeljan *et al.*, "The Impact of Elevated Printing Speeds and Filament Color on the Dimensional Precision and Tensile Properties of FDM-Printed PLA Specimens," *Polymers*, vol. 17, no. 15, Jul. 2025, Art. no. 2090, https://doi.org/10.3390/polym17152090.

[13] L. Changhui *et al.*, "Balanced Optimization of Dimensional Accuracy and Printing Efficiency in FDM Based on Data-Driven Modeling," *Additive Manufacturing Frontiers*, vol. 4, no. 2, Jun. 2025, Art. no. 200220, https://doi.org/10.1016/j.amf.2025.200220.

[14] L. Rihar and E. Hozdić, "Mechanical and Microstructural Response of FDM-Printed PETG and PETG+CF to Variable Infill Architecture and Lubricant Exposure," *Polymers*, vol. 18, no. 5, Mar. 2026, Art. no. 654, https://doi.org/10.3390/polym18050654.

[15] S. Jiang, X. Zhao, H. Liu, and J. Zhu, "Effect of Unit Cell Size on Compressive Strength of 3D-Printed Lattice Structures," in *Proceedings of Chinese Materials Conference 2025*, vol. 106, Y. Chen, Ed. Singapore: Springer Nature Singapore, 2026, pp. 1–8.

[16] M. Daly, M. Tarfaoui, M. Chihi, and C. Bouraoui, "FDM Technology and the Effect of Printing Parameters on the Tensile Strength of ABS Parts," *The International Journal of Advanced Manufacturing Technology*, vol. 126, no. 11–12, pp. 5307–5323, Jun. 2023, https://doi.org/10.1007/s00170-023-11486-y.

[17] M. A. Salman *et al.*, "Effect of Nozzle Diameter and Raster Angle on the Mechanical Properties of 3D Printed Nylon/ Carbon Fibers," *Engineering, Technology & Applied Science Research*, vol. 15, no. 2, pp. 21410–21417, Apr. 2025, https://doi.org/10.48084/etasr.9979.

[18] P. Ferretti *et al.*, "Relationship between FDM 3D Printing Parameters Study: Parameter Optimization for Lower Defects," *Polymers*, vol. 13, no. 13, Jun. 2021, Art. no. 2190, https://doi.org/10.3390/polym13132190.

[19] E. Ceretti, P. Ginestra, P. I. Neto, A. Fiorentino, and J. V. L. Da Silva, "Multi-Layered Scaffolds Production via Fused Deposition Modeling (FDM) Using an Open-Source 3D Printer: Process Parameters Optimization for Dimensional Accuracy and Design Reproducibility," *Procedia CIRP*, vol. 65, pp. 13–18, 2017, https://doi.org/10.1016/j.procir.2017.04.042.

[20] V. E. Kothawade, V. P. Wani, and H. A. Chavan, "A Decision-Making Framework for Selecting Rapid Prototyping Processes in Resource-Constrained Industries Using AHP-GRA," *Engineering, Technology & Applied Science Research*, vol. 15, no. 6, pp. 28687–28692, Dec. 2025, https://doi.org/10.48084/etasr.13905.

[21] I. Khan, A. Al Rashid, and M. Koç, "Machine Learning Prediction of Raster Angle Effects on Mechanical Properties of Extrusion-Based Additively Manufactured Conductive Thermoplastic Polyurethane Composites," *Macromolecular Materials and Engineering*, vol. 311, no. 2, Feb. 2026, Art. no. e00248, https://doi.org/10.1002/mame.202500248.

[22] M. Abas, I. Khan, S. Noor, and F. Ahmad, "Integrated Statistical-Machine Learning Framework for Optimizing Surface Roughness and Impact Strength in PETG FDM," *Progress in Additive Manufacturing*, vol. 11, no. 4, pp. 4383–4402, Apr. 2026, https://doi.org/10.1007/s40964-026-01591-1.

[23] I. Khan, A. Al Rashid, and M. Koç, "Machine Learning, Response Surface Method, Microscopic Analysis, and Optimization for Mechanical Properties of Electrically Conductive Polymer Composite Fabricated via Additive Manufacturing," *Oxford Open Materials Science*, vol. 6, no. 1, Jan. 2026, Art. no. itag004, https://doi.org/10.1093/oxfmat/itag004.

[24] S. Wickramasinghe, T. Do, and P. Tran, "FDM-Based 3D Printing of Polymer and Associated Composite: A Review on Mechanical Properties, Defects and Treatments," *Polymers*, vol. 12, no. 7, Jul. 2020, Art. no. 1529, https://doi.org/10.3390/polym12071529.

[25] J. Torres, J. Cotelo, J. Karl, and A. P. Gordon, "Mechanical Property Optimization of FDM PLA in Shear with Multiple Objectives," *JOM*, vol. 67, no. 5, pp. 1183–1193, May 2015, https://doi.org/10.1007/s11837-015-1367-y.

[26] M. Shbanah, M. Jordanov, Z. Nyikes, L. Tóth, and T. A. Kovács, "The Effect of Heat Treatment on a 3D-Printed PLA Polymer's Mechanical Properties," *Polymers*, vol. 15, no. 6, Mar. 2023, Art. no. 1587, https://doi.org/10.3390/polym15061587.

[27] "SolidWorks." SolidWorks Corporation, Dassault Systèmes, Vélizy-Villacoublay, France, Jan. 2026, [Online]. Available: https://www.solidworks.com/support/free-downloads.

[28] *Plastics — Determination of Tensile Properties Part 1: General Principles*, ISO 527-1:2019, International Organization for Standardization, Geneva, Switzerland, 2019.

[29] "Filament Everfil rPETG S10 Diameter/1.75 mm, Color/Black, Net Weight/1.00kg," *3D Kordo*, 2026. https://kordo.eu/en/product/filament-everfil-rpetg-s10-diam-175mm-color-black-weight-100kg-netto/.

[30] D. G. Zisopol, M. Minescu, and D. V. Iacob, "Research on the Influence of Thermoplastic Extrusion Parameters and Annealing Heat Treatment on the Compressive Strength of Specimens Made from PETG and Recycled PETG," *Polymers*, vol. 18, no. 10, May 2026, Art. no. 1201, https://doi.org/10.3390/polym18101201.

[31] "Minitab." Minitab, LLC, 2026, [Online]. Available: https://www.minitab.com/en-us/.

[32] D. G. Zisopol, M. Minescu, and D. V. Iacob, "A Study on the Evaluation of the Compression Behavior of PLA Lattice Structures Manufactured by FDM," *Engineering, Technology & Applied Science Research*, vol. 13, no. 5, pp. 11801–11806, Oct. 2023, https://doi.org/10.48084/etasr.6262.

[33] D. G. Zisopol, M. Minescu, and D. V. Iacob, "A Study on the Tensile Behavior of Specimens Manufactured by FDM from Recycled PETG in the Context of the Circular Economy Transition," *Engineering, Technology & Applied Science Research*, vol. 14, no. 6, pp. 18681–18687, Dec. 2024, https://doi.org/10.48084/etasr.8927.